Effect of charged donor correlation and Wigner liquid formation on the transport properties of a two-dimensional electron gas in modulation δ-doped heterojunctions

R. Grill
Institute of Physics, Charles University, Ke Karlovu 5, CZ-121 16 Prague 2, Czech Republic

G. H. Döhler
Institut für Technische Physik I, Universität Erlangen, Erwin-Rommel-Strasse 1, D-91058 Erlangen, Germany

(Received 4 May 1998)

We report on the calculation of transport properties of a quasi-two-dimensional electron gas (2DEG) positioned at a GaAs/Al_xGa_{1-x}As interface separated by a thin spacer layer from a moderately δ-doped and only partially depleted donor layer. We show that due to a correlated distribution of charge on the donors the mobility of the 2DEG increases significantly against the case without correlations. The pair correlation function of charged (classical) donors is calculated by Monte Carlo simulations. The Boltzmann equation is solved for a degenerate 2DEG at the interface assuming the scattering on the charged donors in the δ layer as the dominant-scattering mechanism. At low temperatures in the limit of the large filling factor of the donor layer the Wigner condensation is observed and a Bragg-like interference effect on the Wigner lattice is reported. Localization in the 2DEG disturbs the effects at the 2D electron concentration $n_e^{(2)} < 10^{10}$ cm^{-2}. An improved structure for experimental studies is proposed. [S0163-1829(99)01212-6]

I. INTRODUCTION

Modulation-doped semiconducting heterostructures are widely used to create a high-mobility two-dimensional electron gas (2DEG). The spatial separation between a δ-doped donor layer and the 2DEG strongly suppresses electron scattering.[1] The flexibility in the choice of the structure parameters (spacer width, doping concentration, and barrier height) allows one to obtain widely varying properties for the 2DEG. A proper gate structure makes it possible to vary the electron concentration on the heterojunction and the charge occupation of the δ layer.

In this paper we investigate the effect of correlations between the ionized donors. We find that the mobility may become much higher than in the uncorrelated case. This effect is strongest if a Wigner liquid (WL) is formed. For references of Wigner crystallization, see Ref. 2. We also discuss the aspects related with the practical realization of the structure with special emphasis on measurements in the WL regime, and a design for an optimized structure is proposed.

The charge distribution in the doping layer is controlled by Coulomb interaction. At low temperature the electrons in the doping layer occupy the deepest levels of the random potential of the donor impurities. As a consequence the potential fluctuations are smoothed. If a large number of neutral donors is located between two ionized donors the relaxation results in a quasiregular Wigner-liquid-like long-range order. The more or less correlated impurity charge distribution influences the electron scattering, and therefore also the transport properties of the 2DEG.[3–6] Therefore, this structure represents a very suitable tool for the study of electron correlations in the δ-doped layer by investigating the properties of the adjacent 2DEG. The properties of the partially ionized dopants in the 2D structures have been discussed also in papers dealing with δ-doped n-i-p-i superstructures where electrons from n-type doped layer are occupying the acceptors in the p layer.[7–9]

We solve the Boltzmann equation in the relaxation-time approximation. The scattering on correlated charged donors in the δ layer, which is positioned at a well-defined distance from the 2DEG is taken into account as the main scattering mechanism. The screening of the Coulomb interaction by the 2DEG is included. Only one subband is assumed to be occupied. The equilibrium distribution of the charges is obtained by Monte Carlo simulations. Results for a GaAs/Al_xGa_{1-x}As heterostructure are presented. The procedure represents a two-dimensional version of a calculation for compensated bulk semiconductors reported in (Ref. 10).

II. THEORY

The heterojunction is assumed to be located at $z=0$. The 2DEG is in a potential well at $z \geqslant 0$ and a δ-doped donor layer is positioned at $z=-z_0 \leqslant 0$ as illustrated in Fig. 1. The dielectric constant ε is medium independent. The energy dispersion of the conduction band is parabolic with an effective mass m. $n_D^{(2)}$, $n_{D^+}^{(2)}$, $n_e^{(2)}$, and $n_{depl}^{(2)}$ are the sheet concentrations of donors and charged donors in the δ layer and of electrons in the 2DEG and the fixed space charges in the depletion layer, respectively. $n_{D^+}^{(2)} = n_e^{(2)} + n_{depl}^{(2)}$ is assumed throughout this paper. The possibility $n_{D^+}^{(2)} \neq n_e^{(2)} + n_{depl}^{(2)}$ can be realized by an additional charge source as it will be discussed later in the paper.

Within the doped layer, the impurities are randomly distributed. In the case of sufficiently weak doping, quantum-mechanical effects due to wave-function overlap of localized impurity states are small and can be neglected. The dopants are assumed to form hydrogenlike states and DX^- states are not considered. The spatial correlations among charged donors $DX^- - d^+$ in detail studied in Refs. 4–6 give another

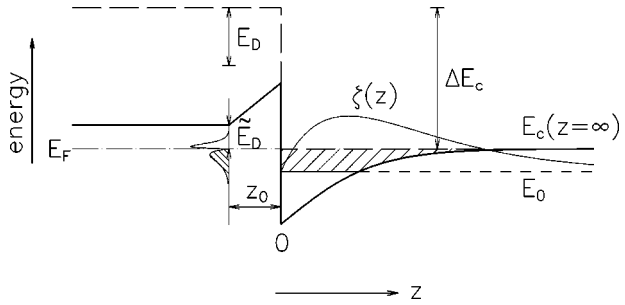

FIG. 1. Schematic diagram of the conduction-band profile without background doping. The dashed line shows the flat band case before charge transfer from the δ layer to the 2DEG. The thick full line is for the equilibrium. The donor energy level changes during the relaxation ($E_D \rightarrow \tilde{E}_D$). The symbols are defined and discussed in the text.

possibility to form the high-mobility 2DEG in modulation-doped structures. The shortcoming of such eventuality consists in annealing temperature $T_a > 100$ K at which the DX^- states are fixed. At such high temperature the long-range spatial correlations cannot develop.

The transition to the acceptor δ doping and to the hole gas at the heterojunction is obvious. The *p*-type doping is advantageous from the point of view of the temperature stability of the correlations. Due to the stronger localization of the acceptor wave functions the doping concentration can be increased and the correlations are then more stable at the higher temperature.

The spatial density of the 2DEG is modulated by interaction with the charges in the δ-doped layer. These modulations generate an additional electrostatic potential, which in turn screens the donor-donor Coulomb interaction. Following Ref. 11 we express the screened potential in the two-dimensional Thomas-Fermi model for degenerate electrons in a triangular potential well here in which

$$\varphi(r,-z_0)=\frac{e}{4\pi\varepsilon\varepsilon_0}\left[\frac{1}{r}-K(r,-z_0)\right], \tag{1}$$

where

$$K(r,-z_0)=q_s\int_0^\infty J_0(qr)\frac{b^6}{(b+q)^6}\frac{e^{-2qz_0}}{q+q_sP_{av}}dq. \tag{2}$$

$J_0(qr)$ is the Bessel function of the first kind of the order zero.[12] The confinement parameter b specifies the envelope wave function in the z direction of the first electronic subband

$$\zeta_0(z)=\sqrt{\frac{b^3}{2}}ze^{-(1/2)bz}. \tag{3}$$

The parameters b, q_s, and P_{av} are the same as given in Ref. 11.

The equilibrium distribution of the charges in the δ layer with an area $\Omega=L^2$, containing $N_D=n_D^{(2)}\Omega$ donors is obtained by a numerical simulation. The MC simulation is done in just the same way as presented in Ref. 10.

The distribution of the charges in the δ layer is characterized by one-particle radial pair-correlation function

$$C_{DD}(r<L/2)=\frac{1}{2\pi r n_{D^+}^{(2)}\Omega}\left\langle\left\langle\sum_{\substack{ij\\ i\neq j}} n_in_j\delta(r-r_{ij})\right\rangle\right\rangle$$

$$C_{DD}(r>L/2)=n_{D^+}^{(2)} \tag{4}$$

and its Fourier transform

$$B(q)=2\pi\int_0^\infty rJ_0(qr)C_{DD}(r)dr$$

$$=2\pi\int_0^{L/2} rJ_0(qr)[C_{DD}(r)-n_{D^+}^{(2)}]dr. \tag{5}$$

$\langle\langle\ldots\rangle\rangle$ means the configuration averaging, n_i is the charge occupation number, and r_{ij} is the donor-donor distance reduced to periodic-boundary conditions.[13] We assume that the charge is fully screened at $r>L/2$.

Due to the homogeneity at large Ω both the functions $C_{DD}(r)$ and $B(q)$ are radial. However, the finite-size effects could partially disturb the results performing numerical calculations. To estimate this artifact we will also calculate the ''direction dependent'' Fourier transform of the charged-donor correlation in the periodic medium

$$\tilde{B}(\mathbf{q})=\frac{1}{n_{D^+}^{(2)}\Omega}\left\langle\left\langle\sum_{\substack{jm\\ j\neq m}} n_jn_m\exp[i\mathbf{q}\cdot(\mathbf{r}_j-\mathbf{r}_m)]\right\rangle\right\rangle, \tag{6}$$

where $\mathbf{q}=2\pi(n_1,n_2)/L$ fulfills the boundary conditions for any integers n_1,n_2.

A. Electron mobility in the 2DEG

The square of the matrix element for the electron scattering on the correlated charges has the form

$$|M(q)|^2=\left(\frac{e}{\Omega}\overline{A}_q\right)^2 n_{D^+}^{(2)}\Omega[1+B(q)], \tag{7}$$

with $B(q)$ from Eq. (5) describing the charged-donor correlation and $\overline{A}_q$ being from Ref. 11. Consequently, the inverse momentum-relaxation time is

$$\frac{1}{\tau(k)}=\frac{m\Omega}{\pi\hbar^3}\int_0^\pi(1-\cos\alpha)|M(k\sqrt{2(1-\cos\alpha)})|^2d\alpha. \tag{8}$$

At sufficiently low temperature when the quasiparticle energy $E(k_F)=\hbar^2k_F^2/2m \gg k_BT$ the approximating form for degenerate electron gas $\langle\tau\rangle=\tau(k_F)$ can be used ($k_F=\sqrt{2\pi n_e^{(2)}}$ is the Fermi wave vector.) For the sake of simplicity we use this approximation in our calculations. In GaAs the condition reads $n_e^{(2)}(\mathrm{cm}^{-2}) \gg 2\times10^9$ T(K).

The final low-temperature form for μ does not contain the temperature explicitly. If all the donors are ionized, there is no donor-donor correlation and $B(q\neq0)=0$. Then μ is temperature independent in this approximation. In case of partly ionized donors in the δ layer the charges relax to an equilibrium state. With increasing temperature the correlated distribution becomes strongly disturbed, even at rather low temperatures, because of the small difference of single-site energies. The scattering of electrons in the 2DEG on more or

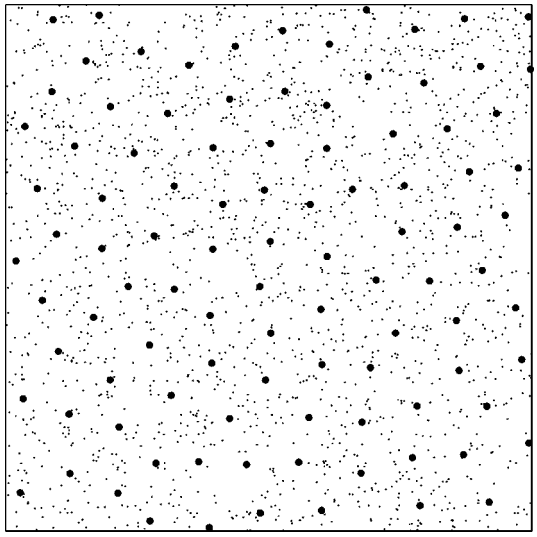

FIG. 2. The formation of a Wigner liquid for $F=0.95$ and $T=0$ K. Dots and bullets indicate neutral donors and positive donors, respectively.

less correlated charged impurities influences the relaxation time significantly. In this way a strong temperature dependence enters into our calculations of the mobility μ.

In the limit of the large filling factor of the donor layer $F=1-n_{D^+}^{(2)}/n_D^{(2)}\to 1$ and for $T\to 0$ K the few remaining charged donors on the donors are forming a Wigner-liquid with a quasiregular hexagonal lattice (see Fig. 2). Simple analytical calculations indicate to us the interesting results that can be found in this limit also on real structures. The lattice constant l and basis vectors $\mathbf{a}_1,\mathbf{a}_2$ of the Wigner lattice are in the form

$$l=\frac{\sqrt{2}}{\sqrt{\sqrt{3}n_{D^+}^{(2)}}}, \tag{9}$$

$$\mathbf{a}_1=l(1,0); \quad \mathbf{a}_2=l\left(\frac{1}{2},\frac{\sqrt{3}}{2}\right). \tag{10}$$

The reciprocal space is then defined by the reciprocal lattice vectors

$$\mathbf{g}_1=\frac{2\pi}{l}\left(-1,\frac{1}{\sqrt{3}}\right); \quad \mathbf{g}_2=\frac{2\pi}{l}\left(0,\frac{2}{\sqrt{3}}\right). \tag{11}$$

If the real structure approaches the WL limit, the $C_{DD}(r)$ shows the δ function like maxima near the values given by the magnitude of the linear combinations of the vectors $\mathbf{a}_1,\mathbf{a}_2$. The corresponding Fourier transform has its maxima in reciprocal space within the linear combinations of $\mathbf{g}_1,\mathbf{g}_2$. The first maximum is at

$$q_{max}=\frac{2\sqrt{2}\pi}{\sqrt[4]{3}}\sqrt{n_{D^+}^{(2)}}=6.752\sqrt{n_{D^+}^{(2)}}. \tag{12}$$

Based on this result we expect an interesting density dependence of the mobility. The argument in M in the upper limit of integration (8) reaches the value $2k_F=5.013\sqrt{n_e^{(2)}}$. If $2k_F<q_{max}$ the integral in (8) is low, and thus the mobility is high. With increasing $n_e^{(2)}$ or decreasing $n_{D^+}^{(2)}$ the opposite relation can be reached and a fast decrease of μ will be observed. This reshaping corresponds to complete filling of the lowest band of the ideal 2D Wigner lattice and a strong scattering at the boundary of its Brillouin zone. In our case without additional source of electrons, $n_e^{(2)}\leqslant n_{D^+}^{(2)}$ and the high mobility regime is established.

If the δ-doped layer is placed near the heterojunction and the temperature is low the electrons can be bound at the potential fluctuations at the interface and the mobility is significantly decreased by this effect. The problems related with the localization and the metal-insulator transition (MIT) in heterostructures have been discussed in the literature.[11,14,15] The critical electron density $n_{ec}^{(2)}$ for the MIT in $Al_xGa_{1-x}As/GaAs$ heterostructures with large spacer width and an ideal 2DEG ($b\to\infty$) has been estimated in[15]

$$n_{ec}^{(2)b}=\frac{\sqrt{n_{D^+}^{(2)}}}{4\sqrt{\pi}z_0}. \tag{13}$$

If the 2DEG confinement becomes comparable with z_0 for thinner spacer layers the value of $n_{ec}^{(2)}$ from Eq. (13) overestimates the actual critical-electron density. Although a study of the MIT is beyond the scope of this paper we develop a simple procedure to estimate the localization in the 2DEG and to get limits of an applicability of the free-electron approximation (Appendix I). A theory of bound states associated with *n*-type inversion layers on silicon, which is similar to our approach, is reported in Ref. 16.

III. RESULTS AND DISCUSSION

The numerical simulations were performed for $GaAs/Al_xGa_{1-x}As$ heterostructures with $m=0.06m_0$ and $\varepsilon=12.5$, which corresponds to $q_s=0.1817$ nm^{-1}. $n_D^{(2)}=2\times 10^{11}$ cm^{-2} was chosen as a proper concentration sufficiently high but below the MIT in the δ layer. The filling factor $F=1-n_{D^+}^{(2)}/n_D^{(2)}$, T, $n_{depl}^{(2)}$, and z_0 were varied and correlation functions were calculated by the MC simulations. The zero temperature configuration has been established as a ''pseudo ground state''[7] in each configuration. Possible procedures to obtain lower minima are analyzed in Ref. 17. We believe that the mobility at the absolute-energy minimum configuration will not be very different from our results. We assume that the tunneling between donors in the δ layer and the 2DEG allows us to reach the thermodynamic equilibrium also at low temperature. For details see Ref. 3. The charge relaxation can be studied by the time-scale response of the mobility to a gate voltage or a sample irradiation.

The calculations were made on cells of various size to estimate the influence of finite-size effects. As an optimum a cell of 1000 donors, corresponding to $L=7.07\times 10^{-5}$ cm was found. In this case the Coulomb interaction is sufficiently screened at the distance $L/2$ to reduce the finite-size effects. Simultaneously the system is not too large and fast calculations are possible. For $F\geqslant 0.90$ a cell of 2000 donors was used. The screening of the Coulomb interaction is illustrated in Fig. 3 by showing the function $rK(r,-z_0)$ [Eq. (1)]. $rK(r,-z_0)=1$ is equivalent to the total screening of the interaction. We see that the interaction is effectively

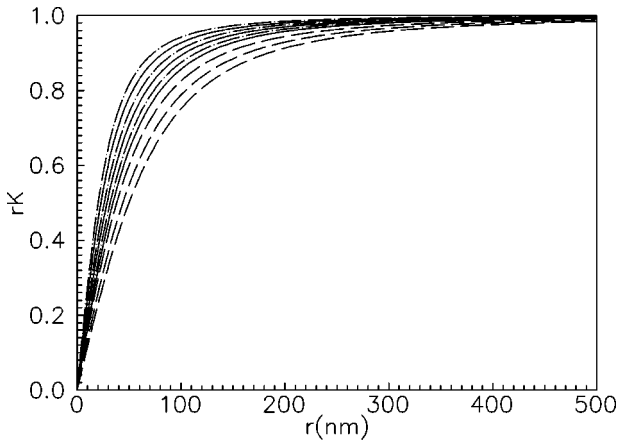

FIG. 3. Screening function $r \cdot K(r,-z_0)$. Dashed lines correspond to $n_{D^+}^{(2)}=10^{10}$ cm^{-2} ($b=77.8$ μm^{-1}), full lines to $n_{D^+}^{(2)}=10^{11}$ cm^{-2} ($b=167.6$ μm^{-1}) and dashed-dotted lines to $n_{D^+}^{(2)}=1.9\times10^{11}$ cm^{-2} ($b=207.6$ μm^{-1}). The same line type shows gradually $z_0=15$, 10, and 5 nm in the direction to the left upper corner. $n_{depl}^{(2)}=0$ in all cases.

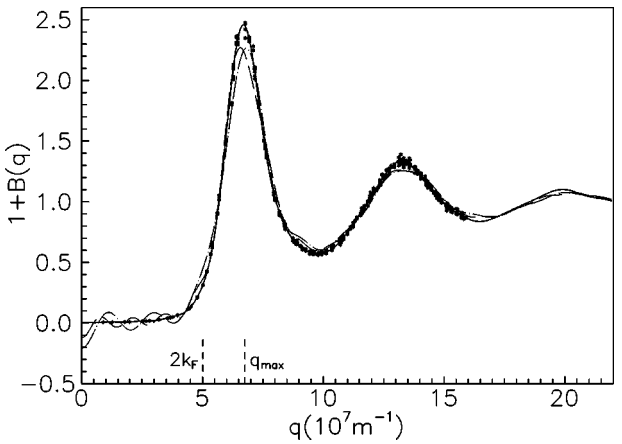

FIG. 5. The Fourier transform $B(q)$ of $C_{DD}(r)$ for screened potential [$n_D^{(2)}\Omega=2000$, full lines] and unscreened potential [$n_D^{(2)}\Omega=2000$; dashed lines; $n_D^{(2)}\Omega=1000$; dash-dotted lines] at $T=0$ K, $F=0.95$. The screened $n_D^{(2)}\Omega=1000$ case exhibits insignificant deviations compared with the full line. The points correspond to the direction-dependent $\tilde{B}(\mathbf{q})$ for the screened case at $n_D^{(2)}\Omega=1000$. The labels $2k_F$ and q_{max} have been introduced in Sec. II A.

screened within $r\approx100-200$ nm for all the considered configurations.

Figure 4 shows a typical set of radial pair-correlation functions $C_{DD}(r)$ with F as a parameter calculated for $z_0=10$ nm, $n_{depl}^{(2)}=0$, and $T=0$ K (full lines) and $T=2$ K (dashed lines). The high F's with well-resolved oscillations correspond to the WL regime. Due to the strong temperature dependence the transport measurements have to be performed at temperatures as low as possible. The oscillations at the lower F's are less pronounced but more stable than those at the higher ones. In the case of low F the electrons occupy the lowest levels of the random potential and the long-range order is destroyed. These configurations are stable in temperature. The $C_{DD}(r)$ functions at other z_0 values do not exhibit significant change compared to Fig. 4.

The influence of screening of the Coulomb potential was studied for $C_{DD}(r)$ as well as for its Fourier transforms $B(q)$ and $\tilde{B}(\mathbf{q})$ from Eqs. (5) and (6) by comparing the results for the screened and the unscreened case $K(r,-z_0)=0$. At the $C_{DD}(r)$ we did not see significant differences except for the peculiar fact that the oscillations in the unscreened case are slightly less pronounced.

More remarkable effects are observed in the Fourier transform (5) depicted in Fig. 5. The unscreened $B(q)$ contains additional Ω-dependent oscillations at small q, which indicate a long-range size-dependent ordering. The points in Fig. 5 correspond to screened (direction dependent) $\tilde{B}(\mathbf{q})$. A very good agreement with related $B(q)$ is obtained.

The most surprising results were observed at the unscreened $\tilde{B}(\mathbf{q})$. Due to the discrete values of $\mathbf{q}$ we present the results in Fig. 6 as the points for single q together with the lines obtained for the same parameters from the calculations of $B(q)$. The circled points correspond to the q's perpendicular to the boundaries $\mathbf{q}=2\pi(n,0)/L$ and $\mathbf{q}=2\pi(0,n)/L$. The odd and even n values yield the data points below and above the lines. The significant deviations

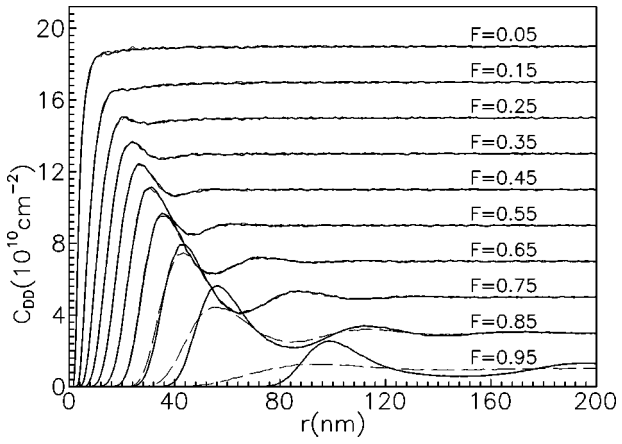

FIG. 4. The correlation functions $C_{DD}(r)$ for various filling factors F at $z_0=10$ nm and $n_{depl}^{(2)}=0$. The full lines correspond to $T=0$ K, the dashed lines to $T=2$ K.

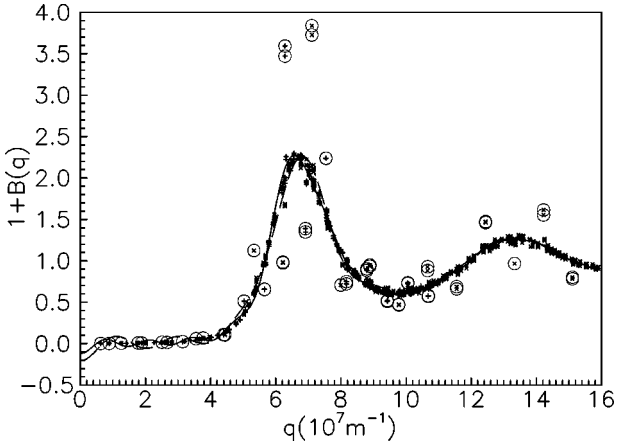

FIG. 6. The Fourier transform $B(q)$ and $\tilde{B}(\mathbf{q})$ for the unscreened potential. Full line and (+) correspond to $n_D^{(2)}\Omega=2000$, dashed line and ($\times$) to $n_D^{(2)}\Omega=1000$. $T=0$ K, $F=0.95$. Circled points are described in the text.

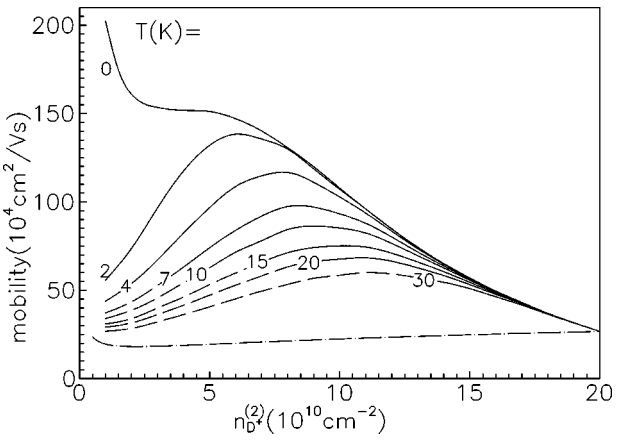

FIG. 7. Electron mobility versus ionized donor density electron density $n_e^{(2)}=N_{D^+}^{(2)}$ for $z_0=10$ nm. The labels at the lines indicate the temperature. The dashed parts of the curves left of the labels show the region where $E(k_F)<2k_BT$ and the 2DEG cannot be assumed as degenerate. The plots are thus only approximative there. The dash-dotted line was calculated without correlations, i.e., $B(q)=0$. $n_{D^+}^{(2)}=20\times10^{10}$ cm^{-2} corresponds to $F=0$.

of the circled points from the direction-averaged $B(q)$ indicate that additional charge modulations with square symmetry are created. These finite-size effects disturb the correct results if the Coulomb interaction is not screened at $r<L/2$. A similar behavior was reported also in Ref. 9 and for three-dimensions in Ref. 10. Deviations for other directions of q were not observed. The question for the subsequent discussion remains how these effects influence the density of states and especially the Coulomb gap formation in this case. The unscreened Coulomb interaction is often used for the study of a Coulomb glass model of interacting localized electrons in a random potential.[18]

The number of averaged configurations was chosen sufficiently high to ensure a relative error of μ of less than 0.25%. A faster convergency was found at higher temperatures. In Fig. 7 plots of μ as a function of increasing ionized donor density and correspondingly also electron density in the 2DEG are shown. [$n_{D^+}^{(2)}=n_e^{(2)}$ here.] This corresponds to an electron transfer from the δ layer to the 2DEG due to a change of gate bias, e.g. The results are given for various temperatures with $z_0=10$ nm. We can distinguish two basic characteristics there. The low $n_{D^+}^{(2)}$ range corresponds to the highly ordered structure. As shown in Fig. 4 the degree of order is strongly temperature dependent, being more stable at higher $n_{D^+}^{(2)}$. The increase of the zero temperature μ at low $n_{D^+}^{(2)}$ is caused by significant ordering and Wigner condensation in that case. $\mu(T=0)$ converges to infinity at $F\rightarrow1$. This effect, however, will hardly be observed experimentally. Localization will play an important role at $F\rightarrow1$ and also other scattering mechanisms will compete to keep the value of μ finite.

In the high $n_{D^+}^{(2)}$ range of Fig. 7 we observe the decrease of μ due to increasing density of scattering centers, increasing confinement of the 2DEG and increasing potential fluctuations. The comparison with the case without correlations shows that the first two effects are certainly too weak to explain this finding. This range of low filling factors is easily

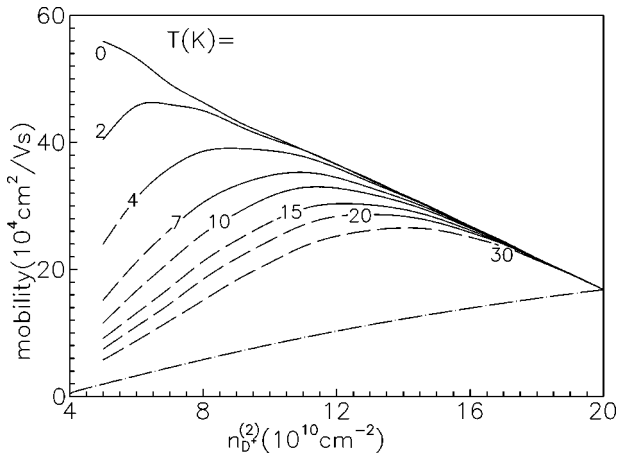

FIG. 8. The electron mobility versus ionized donor density for $n_{depl}^{(2)}=4\times10^{10}$ cm^{-2} and $n_e^{(2)}=n_{D^+}^{(2)}-n_{depl}^{(2)}$ for $z_0=10$ nm. The line description is identical with that in Fig. 7.

accessible for measurements. The strong decrease of μ also at higher temperatures simplifies the experimental setup and evokes an anomalous behavior of the conductivity, which decreases when the concentration of the 2DEG increases.

The more realistic case for $n_{depl}^{(2)}=4\times10^{10}$ cm^{-2} corresponding to $\approx10^{14}$ cm^{-3} background acceptor concentration is presented in Fig. 8. We observe a similar $n_{D^+}^{(2)}$ dependence of μ as in Fig. 7 but the mobilities are generally significantly lowered. The WL regime and high filling factors $F>0.8$ cannot be reached here.

We have observed that the correlation functions are strongly dependent on T and F, but they are only slightly influenced by screening of the Coulomb interaction. This result is convenient for an appreciable simplification of the numerical calculations. $C_{DD}(r)$ can be calculated for one typical choice of the parameters and afterwards used for the calculations of μ in a wide interval of z_0 and b. We illustrate this fact in Fig. 9 where we plot $\mu(T=2$ K,$z_0=10$ nm) calculated with $B(q)$ [Eq. (5)] taken from simulations at $T=2$ K and three different values of $z_0=5$, 10, and 15 nm. Similar results were obtained also for other z_0 and T including $T=0$ K. In case of variable $n_D^{(2)}$ at constant F the charge

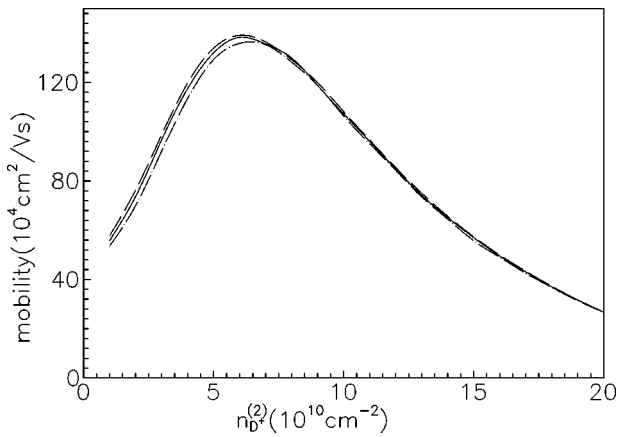

FIG. 9. The electron mobility for $T=2$ K and $z_0=10$ nm calculated using correlation functions at $z_0=5$ nm (dash-dotted), 10 nm (full), and 15 nm (dashed).

TABLE I. The effective radius a^*, the binding energy E_α, and the critical concentration $n_{ec}^{(2)a}$ for the ideal 2DEG ($b\to\infty$) and $n_{ec}^{(2)b}$ for $n_{depl}^{(2)}=0$ left column and $n_{depl}^{(2)}=4\times10^{10}$ cm^{-2} right column as a function of the δ-layer distance z_0.

z_0 (nm)	a^* (nm)	E_α (meV)	$n_{ec}^{(2)a}$ (10^{10} cm^{-2})	$n_{ec}^{(2)b}$ (10^{10} cm^{-2})	
5	17.4	8.3	4.3	7.9	10.9
10	24.6	5.2	2.1	2.0	4.0
15	30.6	3.9	1.4	0.88	2.4
20	36.0	3.2	1.0	0.50	1.7

distribution is determined by a length unit $1/\sqrt{n_D^{(2)}}$ and by a coupling constant of the temperature-activated hopping process $e\varphi(1/\sqrt{n_D^{(2)}},-z_0)/k_BT$. In view of these arguments the C_{DD} at various $n_D^{(2)}$ can be obtained using the approximative relation

$$C_{DD}(r,n_{D2}^{(2)},F,T)\approx C_{DD}\left(r\sqrt{\frac{n_{D2}^{(2)}}{n_{D1}^{(2)}}},n_{D1}^{(2)},F,T\sqrt{\frac{n_{D1}^{(2)}}{n_{D2}^{(2)}}}\right)\frac{n_{D2}^{(2)}}{n_{D1}^{(2)}}. \tag{14}$$

C_{DD} is independent of $n_e^{(2)}$ if only one subband is populated.

In order to estimate the critical density for the MIT in the 2DEG Eq. (A4) was solved (see the Appendix) and the effective radius a^*, the critical concentration $n_{ec}^{(2)a}$, and binding energy E_α were calculated. A comparison with the critical concentration $n_{ec}^{(2)b}$ obtained according to Eq. (13) was also made. The results for the ideal 2DEG are presented in Table I. Both versions of $n_{ec}^{(2)}$ are in qualitative agreement pointing to localization at $n_e^{(2)}\sim10^{10}$ cm^{-2}.

The results for the real 2DEG (b finite) and $n_{depl}^{(2)}=4\times10^{10}$ cm^{-2} are given in Table II. The MIT occurs at $n_e^{(2)}=n_{ec}^{(2)a}$, it means $n_{ec}^{(2)a}=1.1\times10^{10}$ cm^{-2} for $z_0=5$ nm and $n_{ec}^{(2)a}=0.64\times10^{10}$ cm^{-2} for $z_0=15$ nm. The finite width of the 2DEG weakens the binding to the impurity; however, the localization influences the system in this case at low $n_e^{(2)}$, too. We conclude that the localization provides a serious complication for the determination of μ in the WL regime.

The important point of designing this structure is a careful choice of the $Ga_xAl_{1-x}As$ composition to set a proper conduction band offset ΔE_c to reach the favorable starting F. The standard procedure gives (see Fig. 1)

$$\Delta E_c=\tilde{E}_D+\frac{e^2n_{D^+}^{(2)}}{\varepsilon\varepsilon_0}z_0+E_0+\frac{\pi\hbar^2n_e^{(2)}}{m}. \tag{15}$$

The second term results from the space-charge potential in the wide-gap material and the fourth term expresses the Fermi energy of the 2DEG $E(k_F)$. If the background doping is negligible the alternative formula is applicable

$$\Delta E_c=\tilde{E}_D+\frac{e^2n_{D^+}^{(2)}}{\varepsilon\varepsilon_0}\left(z_0+\frac{3}{b}\right). \tag{16}$$

The deviation of the donor level $\tilde{E}_D$ from E_D results from the relaxation of the charge to lower levels of the impurity band. The single-site energy expresses the energy as a sum of energy of the Coulomb interaction with the charged donors and with the 2DEG. In the case without relaxation the electrons on donors are distributed randomly and their mean interaction energy is expressed by the standard formula

$$E_I=-\frac{e^2n_{D^+}^{(2)}}{\varepsilon\varepsilon_0}\left(z_0+\frac{3}{b}\right). \tag{17}$$

In the case after relaxation at $T=0$ K the occupied and unoccupied states are separated energetically by the Coulomb gap. The difference of the E_I and the Coulomb-gap position E_{Coul} gives the variation of the donor level $\Delta E_D=\tilde{E}_D-E_D=E_I-E_{Coul}$. The width of the Coulomb gap is negligible in our calculations and a better specification of ΔE_D in this respect is meaningless.

The resulting ΔE_D is shown in Fig. 10. Due to the neglected background doping in Fig. 1 the bands are flat on the left of the δ layer and on the right of the 2DEG. If background doping is present the bands are bent outside the structure to reach the background activation energy at $z=\pm\infty$. If a 2DEG at the heterojunction exists, the energy shift con-

TABLE II. The effective radius a^*, the critical concentration $n_{ec}^{(2)a}$, and the binding energy E_α for $n_{depl}^{(2)}=4\times10^{10}$ cm^{-2} as a function of n_e or corresponding confinement parameter b.

		$z_0=5$ nm			$z_0=15$ nm		
b (μm^{-1})	n_e (10^{10} cm^{-2})	a^* (nm)	$n_{ec}^{(2)a}$ (10^{10} cm^{-2})	E_α (meV)	a^* (nm)	$n_{ec}^{(2)a}$ (10^{10} cm^{-2})	E_α (meV)
181	1	34.4	1.10	3.25	45.0	0.64	2.32
195	4	33.4	1.15	3.38	44.2	0.66	2.38
210	8	32.6	1.22	3.51	43.2	0.69	2.44
223	12	31.8	1.28	3.62	42.6	0.71	2.49
235	16	31.2	1.33	3.71	42.2	0.73	2.54

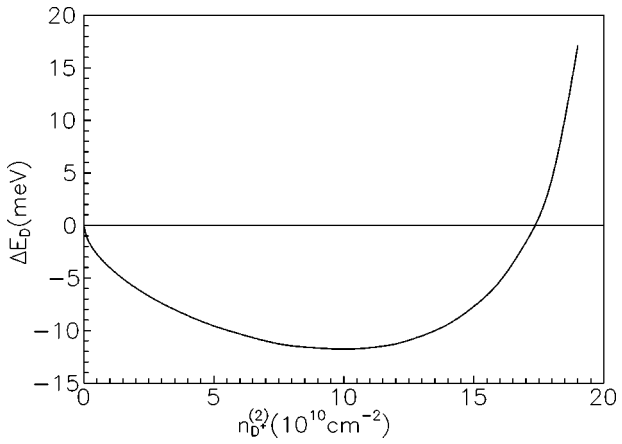

FIG. 10. The variation of the donor energy level due to the charge relaxation in the 2D classical impurity band. One configuration with $n_D^{(2)}\Omega = 16\,000$ was calculated for any $n_{D^+}^{(2)}$.

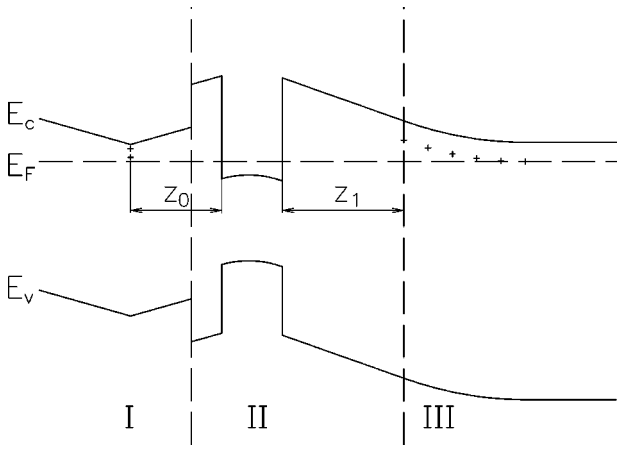

FIG. 11. The scheme of the structure for the WL measurements.

nected with additional band bending does not affect the character of ΔE_D. The fast increase of ΔE_D at high $n_{D^+}^{(2)}$ (low F) is caused by filling only the lowest tail states of the donor impurity band [$\Delta E_D(F \to 0) \to +\infty$ in our model of a classical impurity band]. Due to this fact the realization of the structure with completely charged impurities without any correlations is impossible. A similar behavior of the classical impurity band was also reported for $\delta - n - i - p - i$ structures.[7]

Equation (16) reveals another problem of the present structure with regard to measurements of the WL. ΔE_c is very low in this case. The required height of the barrier between donors and the 2DEG is given practically by $\Delta E_c \approx \tilde{E}_D < E_D$ here. The overlap between doping and free states plays a significant role and μ is influenced by that.

IV. THE RECOMMENDATIONS AND DESIGN IMPROVEMENT TO ENABLE THE WL MEASUREMENT

The value of z_0 in the range from 10 to 15 nm looks optimum for the magnitude of μ. Samples with $\mu \approx 10^6$ cm^2/V s are currently prepared by molecular beam epitaxy (MBE). At $z_0 = 5$ nm the mobility decreases approximately by a factor of 2 compared with that at $z_0 = 10$ nm. The transport properties at low z_0, however, will be influenced by the hybridization of the electrons in the 2DEG with the impurity states and by strong localization. The distance larger than $z_0 \approx 15$ nm yields $\mu > 3 \times 10^6$ cm^2/V s at low temperatures. These high values approach to the present technological limit on such structures and other scattering mechanisms may obscure the expected behavior. If measurements at low F are intended the increase of z_0 to $15-20$ nm is recommended. In this case also $n_D^{(2)}$ can be increased because the MIT occurs at higher F.

We shall discuss now the possibilities on how to improve this simple structure in order to avoid its drawbacks and to allow measurements as a function of both varying $n_{D^+}^{(2)}$ and $n_e^{(2)}$, including the WL regime. We set the following requirements: (i) the 2DEG should be confined to the region close to the δ layer to intensify the scattering on that, (ii) z_0 should be large to minimize the localization, (iii) the potential barrier should be high to keep the overlap of the electron subband states with the donor states small, and (iv) an additional electron source should be present to compensate for the electrons lost in the background doping and to allow for independent tuning of $n_{D^+}^{(2)}$ and $n_e^{(2)}$.

To fulfill the above conditions we propose the structure schematically depicted in Fig. 11. It consists of a narrow quantum well (II) in a wide gap material, which reduces the penetration outside the well. The δ-doped layer (I) is placed in a more narrow gap material to fit the proper equilibrium filling factor F. The additional charge source (III) is achieved by an n-doped layer in the wide gap material, which is distant enough to suppress the scattering on the charged donors in it ($z_1 \gg z_0$). The charge transfer between the regions is achieved by applying independently suitable gate voltages between contacts to the 2DEG and the front and the back gate.

The most interesting result expected at this structure can be deduced from the oscillating form of $B(q)$ (Fig. 5). The possibility to vary $k_F[n_e^{(2)}]$ without changing F allows us to sweep $B(q)$ along the oscillations. For a simple preliminary illustration we have calculated μ for structure composed of a δ-doped single heterojunction with a confinement parameter $b = 600\ \mu\text{m}^{-1}$ and independent variation of $n_{D^+}^{(2)}$ and $n_e^{(2)}$. The results are shown in Fig. 12 as a surface plot $\mu[n_{D^+}^{(2)}, n_e^{(2)}]$. The peak at low $n_{D^+}^{(2)}$ and $n_e^{(2)}$ corresponds to the WL regime. The decrease of μ with increasing $n_{D^+}^{(2)}$ is due to decreasing correlations. The shape of $\mu[n_e^{(2)}]$ at constant values of $n_{D^+}^{(2)}$ reflects the effect of sweeping $2k_F = \sqrt{8\pi n_e^{(2)}}$ through the oscillations of $B(q)$. If $2k_F$ passes the first maximum at $B(q)$, the μ decreases fast and approaches to the case without correlations.

V. CONCLUSIONS

We have shown that the study of electron transport in the δ-doped single heterojunction can reveal an interesting effect of electron correlation in a partially depleted δ layer. The method can be simply used in case of low filling factors when the loss of electrons on the background acceptors does

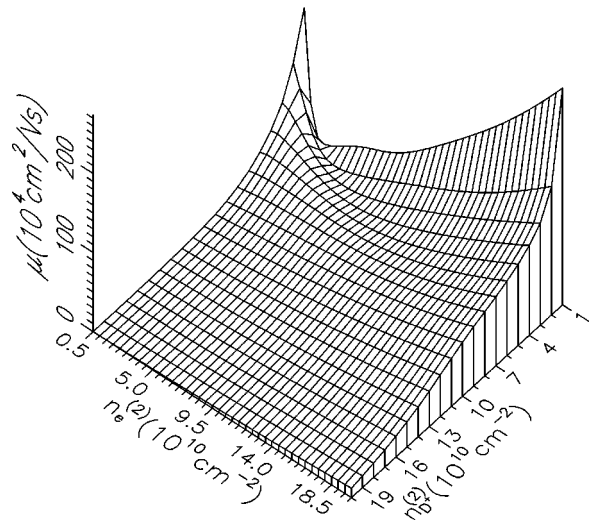

FIG. 12. The presumed course of mobility for recommended structure of quantum well and two doping regions with independent tuning of $n_{D^+}^{(2)}$ and $n_e^{(2)}$. $T=0$ K, $z_0=10$ nm, $b=600\ \mu\mathrm{m}^{-1}$, and $n_{depl}^{(2)}=0$.

not reduce $n_e^{(2)}$ significantly and the band offset ΔE_c can be chosen sufficiently high. A gate voltage or optical excitation allow to vary the electron distribution between the δ layer and the 2DEG. The main effect to be observed is the decrease of the conductivity of the 2DEG with increasing $n_e^{(2)}$ (decreasing F).

The simple structure is not suitable for measurements at the high filling factor and the Wigner condensation is difficult to be measured due to localization, hybridization with the δ-doping states, and the loss of electrons on the background acceptors. For this case we propose a more sophisticated structure consisting of a quantum well and two doped regions. Higher δ doping is favorable for the observation of the correlation effects. In this case, however, the parallel current in the δ layer has to be considered as well. Perspectively, the correlated structure can be partially disturbed by the gate voltage and temperature variation or optically and ensuing time-scale measurements of the mobility can prove the charge relaxation in the δ layer. The questions mentioned in Ref. 3 can be by this way elucidated.

The same effects can be also studied on a system of two-dimensional hole gas and the adjacent acceptor δ-doped layer. In this case a higher δ-doping concentration can be used and consequently a temperature stability of the correlations up to about 8 K is expected.

ACKNOWLEDGMENTS

This paper was financially supported by the Deutschen Akademischen Austauschdienst (DAAD, Bonn, Germany), by the Alexander von Humboldt Foundation (AvH, Bonn, Germany), and by the Ministry of Education of Czech Republic under Grant No. VS97113.

APPENDIX

As a model structure to study the localization in the 2DEG we assume the doping charge homogeneously spread out in the δ layer + one positive charge at $r=0$ in the layer. We consider the system described by the Hamiltonian

$$H=H_0+H_z+U_{imp}. \tag{A1}$$

H_0 corresponds to free-particle motion parallel to the layer, H_z describes quantized states in the one-dimensional quantum well, and U_{imp} is the impurity Coulomb potential

$$U_{imp}=-\frac{e^2}{4\pi\varepsilon\varepsilon_0\sqrt{r^2+(z+z_0)^2}}. \tag{A2}$$

We use the ansatz for a trial wave function

$$\psi(r,z)=\zeta_0(z)\chi(r), \tag{A3}$$

where $\zeta_0(z)$ is the eigenfunction of H_z given by Eq. (3) with the eigenvalue E_0 as the bottom of the occupied subband. Multiplying the Schrödinger equation with the Hamiltonian (A1) by $\zeta_0(z)$ and integrating in z we get the equation for the radial function $\chi(r)$

$$-\frac{\hbar^2}{2m}\left(\frac{\partial^2\chi}{\partial r^2}+\frac{1}{r}\frac{\partial\chi}{\partial r}\right)-\chi\frac{e^2}{4\pi\varepsilon\varepsilon_0}\times\int_0^\infty\frac{|\zeta_0(z)|^2}{\sqrt{r^2+(z+z_0)^2}}dz=(E-E_0)\chi. \tag{A4}$$

Looking for the ground-state (nodeless) solution of Eq. (A4) it is useful to express χ in the exponential form

$$\chi(r)=e^{-s(r)}, \tag{A5}$$

where s is real and positive. After substitution we get

$$s''=(s')^2-\frac{1}{r}s'+\frac{2m}{\hbar^2}[E-E_0+I(r)], \tag{A6}$$

where

$$I(r)=\frac{e^2}{4\pi\varepsilon\varepsilon_0}\int_0^\infty\frac{|\zeta_0(z)|^2}{\sqrt{r^2+(z+z_0)^2}}dz. \tag{A7}$$

Due to the radial symmetry with continuous derivatives $s'(r)$ has to fulfill boundary conditions $s'(r=0)=0$, $s''(r=0)=1/r\,s'(r=0)=m/\hbar^2[E-E_0+I(0)]$, and $s'(\infty)=\mathrm{const}$. Starting the numerical solution from $r=0$ the last condition establishes the eigenenergy E. $E_\alpha=E_0-E$ is then the ionization energy of the bound state.

We assume a hydrogenlike shape of χ and define the effective radius a^* as $\chi(a^*)=\chi(0)/e$ (here e is the Euler constant). Finally, we obtain the critical impurity density from[19]

$$\sqrt{n_{ec}^{(2)a}}a^*=0.36. \tag{A8}$$

The higher concentration corresponds to the metallic side of the MIT.

[1] T. Saku, Y. Horikoshi, and S. Tarucha, Jpn. J. Appl. Phys., Part 1 **33**, 4837 (1994).
[2] H. Kamimura and H. Aoki, *The Physics of Interacting Electrons in Disordered Systems* (Clarendon Press, Oxford, 1989).
[3] A. L. Efros, F. G. Pikus, and G. G. Samsonidze, Phys. Rev. B **41**, 8295 (1990).
[4] E. Buks, M. Heiblum, and Hadas Shtrikman, Phys. Rev. B **49**, 14 790 (1994).
[5] T. Suski, P. Wiśniewski, I. Gorczyca, L. H. Dmowski, R. Piotrzkowski, P. Sobkowicz, J. Smoliner, E. Gornik, G. Böhm, and G. Weimann, Phys. Rev. B **50**, 2723 (1994).
[6] R. Shikler, M. Heiblum, and V. Umansky, Phys. Rev. B **55**, 15 427 (1997).
[7] T. Schmidt, C. Metzner, St. G. Müller, and G. H. Döhler, Phys. Rev. B **47**, 10 633 (1993).
[8] C. Metzner, H. J. Beyer, and G. H. Döhler, Phys. Rev. B **46**, 4128 (1992).
[9] F. A. Reboredo, Phys. Rev. B **51**, 5089 (1995).
[10] R. Grill, J. Phys. Condens. Matter **7**, 3565 (1995).
[11] T. Ando, A. B. Fowler, and F. Stern, Rev. Mod. Phys. **54**, 437 (1982).
[12] F. Stern and W. E. Howard, Phys. Rev. **163**, 816 (1967).
[13] J. H. Davies, P. A. Lee, and T. M. Rice, Phys. Rev. B **29**, 4260 (1984).
[14] J. Serre, A. Ghazali, and A. Gold, Phys. Rev. B **39**, 8499 (1989).
[15] A. Gold, Phys. Rev. B **44**, 8818 (1991).
[16] B. G. Martin and R. F. Wallis, Phys. Rev. B **18**, 5644 (1978).
[17] A. Möbius, M. Richter, and B. Drittler, Phys. Rev. B **45**, 11 568 (1992).
[18] M. Sarvestani, M. Schreiber, and T. Vojta, Phys. Rev. B **52**, R3820 (1995).
[19] B. T. Debney, J. Phys. C **10**, 4719 (1977).